# Frequency Regulation in Hybrid Power Dynamics with Variable and Low Inertia due to Renewable Energy

Patricia Hidalgo-Gonzalez, Roel Dobbe, Rodrigo Henriquez-Auba, Duncan S. Callaway and Claire J. Tomlin

Abstract—As more non-synchronous renewable energy sources (RES) participate in power systems, the system's inertia decreases and becomes time dependent, challenging the ability of existing control schemes to maintain frequency stability. System operators, research laboratories, and academic institutes have expressed the importance to adapt to this new power system paradigm. As one of the potential solutions, virtual inertia has become an active research area. However, power dynamics have been modeled as time-invariant, by not modeling the variability in the system's inertia. To address this, we propose a new modeling framework for power system dynamics to simulate a time-varying evolution of rotational inertia coefficients in a network. We model power dynamics as a hybrid system with discrete modes representing different rotational inertia regimes of the network. We test the performance of two classical controllers from the literature in this new hybrid modeling framework: optimal closed-loop Model Predictive Control (MPC) and virtual inertia placement. Results show that the optimal closed-loop MPC controller (Linear MPC) performs the best in terms of cost; it is 82 percent less expensive than virtual inertia placement. It is also more efficient in terms of energy injected/absorbed to control frequency. To address the lower performance of virtual inertia placement, we then propose a new Dynamic Inertia Placement scheme and we find that it is more efficient in terms of cost (74 percent cheaper) and energy usage, compared to classical inertia placement schemes from the literature.

#### I. INTRODUCTION

In power systems, frequency will deviate from its nominal value when there is a mismatch between electricity generation and consumption [1]. There exists a set of mechanisms to prevent frequency excursions. The first automatic response when frequency starts to deviate is the inertial response. This inertial response is originated from the kinetic energy supplied to the grid by the synchronous generators. This inertia (present in rotating masses of generators and turbines) determines the instantaneous frequency change when imbalances of active power occur. Therefore, more inertia in the system will translate into a slower rate of change of the frequency. As the frequency starts deviating, some generators will respond automatically through governor response [2].

\*This work was supported by the National Science Foundation Graduate Research Fellowships Program, NSF PIRE: Science of Design for Societal-Scale Cyber-Physical Systems (Award Number: UNIV59732), NSF awards 1539585, and 1646612.

Patricia Hidalgo-Gonzalez and Duncan S. Callaway are with the Department of Electrical Engineering and Computer Sciences and the Energy and Resources Group, University of California, Berkeley, CA 94720, USA. [patricia.hidalgo.g, dcal]@berkeley.edu

Roel Dobbe, Rodrigo Henriquez-Auba, and Claire J. Tomlin are with the Department of Electrical Engineering and Computer Sciences, University of California, Berkeley, CA 94720, USA. [dobbe, rhenriquez, tomlin]@berkeley.edu

Governor response or droop control is an automatic control proportional to the frequency deviation. After droop control starts actuating, slower mechanisms (e.g. spinning reserves) participate to restore frequency to its nominal value [2].

It is a crucial aspect for the operation and stability of electrical systems to maintain the grid frequency within acceptable ranges. Nowadays, large shares of renewable energy sources (RES) are being integrated into power systems. Several countries have set ambitious goals for the future to provide more electricity using renewable energy [3] and/or reducing their  $CO_2$  emissions. This global drive will steer the power system to a grid dominated by RES [4]. In this scenario, renewable sources, such as wind and solar, are usually connected to the grid through inverters, which decouple their rotational inertia (if existing) from the grid.

Usually, depending on the configuration of the inverters, no inertial response is delivered to the grid. With this increasing penetration of RES, the global system inertia of the power systems is decreasing and time-varying. This can provoke an increment in the variation of frequency under abrupt changes in generation and demand. If no actions are taken, this can lead to cases in which standard frequency control schemes are too slow to mitigate arising contingencies [5].

A possible solution for this issue is to use RES inverters or large scale storage to provide inertia. This can be done by operating the RES or storage's inverters as virtual inertia (control proportional to the derivative of the frequency), that could allow large penetration of RES without jeopardizing the system's stability [6]. Previous work studying virtual inertia can be found in the literature. In [7], a detailed survey of different virtual inertia techniques, topologies and future directions are presented. [8] introduces the concept of inverters that emulate the response of a synchronous machine. [9] proposes a new controller to address low inertia. This work argues that virtual inertia could amplify noise in an unbounded manner. The work from [10] discusses virtual inertia (or inertia mimicking) by enabling inverter-connected generation units to quickly modify their power output via Model Predictive Control (MPC), mimicking the dynamic response of conventional units. In a similar line of work, [11] studies the effect that changes in inertia have on power system stability, and how to best place devices providing virtual inertia. Most recently [12] studied optimal placement of virtual inertia in different nodes of a network. To the best knowledge of the authors, the body of work around virtual inertia has mostly focused on the effects on the grid and on its optimal allocation. The frequency dynamics have been modeled as a time-invariant system. However, when we take into account the nature of the changes of rotational inertia in the grid, it requires a new modeling framework that represents this time dependence and variability of the system's inertia. Thus, the contributions of this paper are the following:

- We propose a new modeling framework for power system dynamics to simulate a time-varying evolution of rotational inertia coefficients in the network. To do this, we model power dynamics as a hybrid system [13] where each mode corresponds to a rotational inertia regime. At each time step of the simulation the dynamical system mode can switch to a different rotational inertia mode in an exogenous fashion.
- We test the performance of two classical controllers from the literature (optimal closed-loop controller from MPC and virtual inertia placement) in this new hybrid modeling framework.
- We propose a new controller (Dynamic Inertia Placement) to more efficiently address low and variable inertia in the grid.

We conclude that the new modeling framework we develop is necessary to design controllers that address frequency regulation in power systems with high RES penetration. We also find that the optimal linear closed-loop controller (referred as Linear MPC in this paper) performs best in terms of cost and energy injected/absorbed to control frequency. Lastly, we find that our proposed controller for Dynamic Inertia Placement (when modeling dynamics with variable inertia) is more efficient in terms of cost and energy usage than the classical Inertia Placement from the literature.

The rest of the paper is organized as follows: Section II presents the problem formulation, Section III shows simulations from a study case, and finally Section IV concludes with our main findings.

#### II. PROBLEM FORMULATION

A. Power system dynamics as a hybrid system

We consider an electric power network modeled as a graph with N nodes and N(N-1)/2 possible edges connecting them. The swing equation model used for this network is based on [1], where dynamics are given by

$$m_i \ddot{\theta}_i + d_i \dot{\theta} = p_{\text{in},i} - \sum_j b_{ij} (\theta_i - \theta_j), \quad i \in \{1, ..., N\}$$
 (1)

 $m_i$  corresponds to the equivalent rotational inertia in node i,  $d_i$  is the droop control,  $p_{\text{in},i}$  represents the power input at node i,  $b_{ij}$  is the susceptance of the transmission line between nodes i and j, and  $\theta_i$  is the voltage phase angle at node i. The state space representation of the model is given by

$$\begin{bmatrix} \dot{\theta} \\ \dot{\omega} \end{bmatrix} = \begin{bmatrix} 0 & I \\ -M^{-1}L & -M^{-1}D \end{bmatrix} \begin{bmatrix} \theta \\ \omega \end{bmatrix} + \begin{bmatrix} 0 \\ M^{-1} \end{bmatrix} p_{\text{in}}$$
(2)

where the states correspond to the stacked vector of angles and frequencies at each node  $(\theta, \omega) \in \mathbb{R}^{2n}$ ,  $M = \text{diag}(m_i)$  is a diagonal matrix with rotational inertia coefficients, D = 0

diag $(d_i)$  is a diagonal matrix with droop control coefficients,  $p_{\rm in}$  corresponds to the power input, and  $L \in \mathbb{R}^{n,n}$  is the Laplacian of the network. The network Laplacian is defined as  $\ell_{ij} = -b_{ij}$  when  $i \neq j$ , and  $\ell_{ii} = \sum_{i \neq j} b_{ij} + y_{i,s}$ , where  $y_{i,s}$  are all shunt admittances connected at node i.

In the traditional paradigm of power systems, where generation has been dominated by thermal generation, the inertia at each node  $m_i$  has been considered constant. However, in recent years, it has been observed that due to the increase in generation from RES, the rotational inertia in the network has become lower and time-varying [5], [14]. In order to model power dynamics taking into account the variability of inertia at each node, our work proposes a new framework for modeling frequency dynamics. Instead of assuming equation (2) as a time-invariant dynamical system, we propose to model it as a Switched Affine hybrid system [13], where each mode will be given by a predetermined set of values of  $m_i$  at each node. The switching between the different mmodes depends on the current online generators. In this work, the mix of online generators at each time step t is modeled as an exogenous input. Therefore, power dynamics will be given by

$$\begin{bmatrix} \dot{\theta} \\ \dot{\omega} \end{bmatrix} = \begin{bmatrix} 0 & I \\ -M_q^{-1}L & -M_q^{-1}D \end{bmatrix} \begin{bmatrix} \theta \\ \omega \end{bmatrix} + \begin{bmatrix} 0 \\ M_q^{-1} \end{bmatrix} p_{\text{in}}$$
(3)

where  $M_q$  represents the inertia matrix M in the current mode  $q \in \{1,...,m\}$ . The switching between modes can occur from any time step t to t+1, and it is given by a uniform distribution with the following possible outcomes:

- No change of inertia
- Increase of inertia
- Decrease of inertia

Thus, the evolution over time of the matrix  $M_q$  is modeled as a Markov Chain. For simplicity, for a given mode q we assume the same inertia coefficients for all nodes. Section III, subsection A, describes in more detail the assumption on inertia coefficients at the nodes of the network.

Power input at node i, can be expressed as

$$p_{in} = (\delta + u), \quad \delta_i \sim N(0, 0.1) \quad i = 1...N$$
 (4)

where  $\delta$  is a time-varying vector whose components,  $\delta_i$ , are disturbances at each node i (modeled as white noise), and the vector u is the controller (power injection). Thus, equation (3) can be written as

$$\begin{bmatrix} \dot{\theta} \\ \dot{\omega} \end{bmatrix} = \begin{bmatrix} 0 & I \\ -M_q^{-1}L & -M_q^{-1}D \end{bmatrix} \begin{bmatrix} \theta \\ \omega \end{bmatrix} + \begin{bmatrix} 0 \\ M_q^{-1} \end{bmatrix} (\delta + u)$$
 (5)

$$\begin{bmatrix}
\dot{\theta} \\
\dot{\omega}
\end{bmatrix} := A_q \begin{bmatrix}
\theta \\
\omega
\end{bmatrix} + B_q (\delta + u) \tag{6}$$

In this hybrid formulation, the design of the optimal controller u is more complex than in the traditional linear time-invariant (LTI) case. Recent work has shown the relevance of the optimal placement of virtual inertia in the grid [12],

which expanded on previous work that studied the effects of rotational inertia in a network [11]. In this study we build on this work by including the evolution over time of the rotational inertia at each node. Using receding horizon Model Predictive Control we study three different designs for the controller u in equation (5).

## B. Optimal frequency control for low and time-varying rotational inertia coefficients

In order to minimize an objective function with the states and controller as variables, we consider three possible controllers u. In addition, we take into account a constraint to maintain the frequency  $\omega$  at all time t in a predefined safe interval. The receding horizon MPC formulation can be summarized by the following optimization problem:

$$\min_{x(t),u(t)} \int_{t=t_0}^{T} x(t)^{\top} Qx(t) + u(t)^{\top} Ru(t) dt$$
 (7)

s.t. 
$$x(t_0) = x_0$$
 (8)

$$\dot{x}(t) = A_q x(t) + B_q \left( \delta(t) + u(t) \right), \quad t \in (t_0, T)$$
 (9)

$$\underline{b} \le x(t) \le \overline{b}, \quad t \in (t_0, T) \tag{10}$$

$$\delta_i(t) \sim N(0, 0.1), \quad i \in \{1, ..., N\}, \quad t \in (t_0, T) \quad (11)$$

where x is the vector of the states  $(\theta, \omega)$ , u the controller, Q and R are symmetric positive definite matrices,  $t_0$  the initial time, T the final time,  $\underline{b}$  and  $\overline{b}$ , lower and upper bounds for the frequency, and  $x_0$  the initial state. As it was mentioned earlier, the hybrid modes q transition at each time step t using a Markov Chain. We consider three designs for optimal controllers u obtained using receding horizon MPC:

1) Linear MPC:

$$u_i(t)$$
 unconstrained,  $i \in \{1,...,N\}, t \in (t_0,T)$  (12)

2) Inertia Placement [12]:

$$u_i(t) = -M_i \dot{\omega}_i, \quad i \in \{1, ..., N\}, \quad t \in (t_0, T)$$
 (13)

3) Dynamic Inertia Placement:

$$u_i(t) = -M_i(t)\dot{\omega}_i, \quad i \in \{1, ..., N\}, \quad t \in (t_0, T)$$
 (14)

The receding horizon MPC formulation (7) - (12) is classified as a quadratic problem with linear constraints, thus a convex problem. The receding horizon MPC formulation for inertia placement, (7) - (11), (13) and (7) - (11), (14), are non convex problems. To model the first formulation we use CVX [15], [16]. To model the non convex formulations we use the parser YALMIP [17], and solved the optimization problem using an interior point method.

In the case of the Linear MPC formulation, the controller  $u_i(t)$  does not have any constraints imposed. Implying that the feasible set of the Linear MPC formulation and the feasible set of the problem given by (7) - (11) are equivalent. The Dynamic Inertia Placement formulation introduces a new variable  $M_i(t)$ . This new variable needs to be optimized for all nodes i at all time steps t. The controller  $u_i(t)$  is constrained to be equal to  $-M_i(t)\dot{\omega}_i$ , serving as virtual inertia. The fact that the Dynamic Inertia Placement formulation has

TABLE I Parameters for the twelve-bus three-region case study [1],  $\label{eq:table_eq} [11].$ 

Parameter	Value	
Transformer reactance	0.15 p.u.	
Line impedance	(0.0001 + 0.001j) p.u./km	
Base voltage	230 kV	
Base power	100 MVA	
Droop control	1.5 %/%	

an extra set of constraints on  $u_i(t)$  implies that the feasible set of this problem is contained in the feasible set of the Linear MPC formulation. Finally, the Inertia Placement formulation, in addition to having the constraint on the structure of  $u_i(t)$ as the Dynamic Inertia Placement had, it has an additional set of constraints. This extra set of constraints forces  $M_i(t)$  to be equal to  $M_i$  for all t. In other words, the design of the virtual inertia controller cannot be specific to a node and time, but a fixed design over time for each node. Thus, the Inertia Placement formulation has its feasible set contained in the feasible set of the Dynamic Inertia Placement formulation. In summary, the Linear MPC formulation has the largest feasible set, followed by the Dynamic Inertia Placement which has more constraints. Finally the Inertia Placement formulation comes in third place with the most restrictive feasible set. Due to this, we expect solutions  $u^*$  from the Linear MPC formulation to be best, attaining the lowest value in its objective function. We expect the Dynamic Inertia Placement case to come in second place with a higher optimal value for its objective function compared to the Linear MPC formulation. The formulation with the highest optimal value of its objective function would be the Inertia Placement formulation.

One of the contributions of this work is to assess the grid's performance when virtual inertia is optimized over time and location (Dynamic Inertia Placement). We also compare inertia placement with the Linear MPC formulation. The latter sheds light on how the performance of frequency dynamics could improve with a more flexible controller (not constrained to be a derivative control law as inertia placement is).

In Section III we compare these three formulations. We utilize the study case (originally from [1]) used in some recent virtual inertia placement work [11] and [12].

### III. CASE STUDY: TWELVE-BUS THREE-REGION NETWORK

#### A. Data description

The twelve-bus three-region network used in this study has also been used in [1], [11], and [12]. The full network was modeled, without using any simplifications (e.g. no Kron reduction of the graph). Therefore, twelve nodes were modeled with two states each (angle and frequency). Table I shows the parameters of the network.

The positive definite matrices Q and R from the objective function in problem (7) that we use in the case study are the

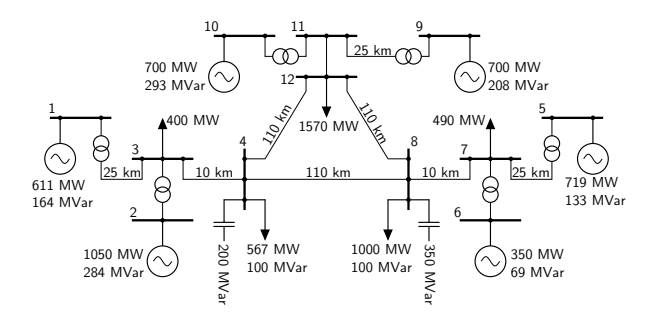


Fig. 1. Case study: Twelve-bus three-region network from [1], [12], and [11].

identities. With this selection we are equally penalizing frequency deviations from zero and energy injection/absorption from the controller. This assumption can be changed to, for example, represent the real economic cost to the grid that frequency deviations and energy injection/absorption from the controller represent. This in itself is an open research question.

As it was discussed in Section II, subsection A, the inertia matrix M is modeled as a diagonal matrix diag $(m_i)$ , whose elements  $m_i$  correspond to the rotational inertia at the bus i. We assume the same rotational inertia in all buses for a given time step t  $(m_i(t) = m(t))$  for all i). This implies a similar fraction of renewable energy generation for all nodes, which is common in large networks. However, this assumption can be easily extended. In this work, we model the variability of the rotational inertia in the system as a hybrid system switching modes as the inertia changes. Each mode of the hybrid system is given by one value of inertia. For the study case we predefined possible inertia values for the system:  $\{0.1, 0.5, 1, 1.5, 2, 2.5, 3, 3.5, 5, 9\}$ . The average of this set of possible inertia values is 2.8 seconds, which is equivalent to having 28 percent of thermal generation (10 s of inertia) and 72 percent of RES with zero inertia. Each simulation starts with 2 seconds of inertia, and from there-based on a uniform distribution draw- the inertia (hybrid mode) of the system at time t+1 will remain the same, increase, or decrease (Markov Chain with 1/3 probability for each possible mode transition). This process is repeated until each time step t in the time horizon T has assigned a rotational inertia mode.

The safety bounds for frequency are  $\pm 0.1$  Hz ( $\underline{b}$  and  $\bar{b}$  in equation (10)).

### B. Results

Each receding horizon MPC formulation is run for eight time steps (T) and 100 possible realizations (or scenarios) from the Markov Chain of the rotational inertia matrix  $M_q$ . Thus, for each formulation we obtain an optimal value of the objective function at each time step and each scenario (i.e. 800 values). The number of nodes, N, is 11 because node 11 and 12 are the same (refer to Fig. 1). We also obtain N control actions (one per node) for each time step and for each scenario (i.e. 8800 values), and N frequency measurements for each time step and for each scenario (i.e. 8800 values). Using these sets of results we calculate moments and show

TABLE II SUMMARY: MEAN AND STANDARD DEVIATION OF OBJECTIVE FUNCTION  $J^*$ , OPTIMAL CONTROL  $u^*$ , AND FREQUENCY  $\omega$ .

Moments	Linear MPC	Inertia Placement	Dynamic Inertia Placement
$\mu(J^*)$	0.17	0.92	0.24
$\sigma(J^*)$	0.07	1.66	0.30
$\mu(u^*)$ p.u.	-0.004	-0.018	-0.005
$\sigma(u^*)$ p.u.	0.13	0.29	0.15
$\mu(\omega)$ mHz	-0.34	0.93	8.10
$\sigma(\omega)$ Hz	0.07	0.04	0.05

histograms for the three formulations in order to compare them.

Table II shows the mean and standard deviation of the set of optimal values of the objective function  $(J^*)$  at all times t and all scenarios for the three formulations. The same moments are shown for optimal control  $(u^*)$  and frequency  $(\omega)$  for the three optimization problems. As discussed in Section II, subsection B, the Linear MPC formulation shows the lowest average and standard deviation values in its objective function compared to the other two formulations. The average of the objective function for the Linear MPC is 0.17 cost units, and its standard deviation 0.07. In the case of the average, it corresponds to 18 percent of the average in the Inertia Placement formulation and 71 percent of the average in the Dynamic Inertia Placement case. This result can be interpreted as the Inertia Placement formulation resulting in non zero frequency deviations and non zero control actions 82 percent more of the time compared to the Linear MPC formulation (on average). This result sheds light on the suboptimality of the virtual (dynamic and static) inertia controllers compared to the closed-loop formulation (Linear MPC). Thus, there is an incentive to continue designing controllers that try to address low and variable inertia coefficients in the grid.

Another relevant result is the fact that our proposed Dynamic Inertia Placement formulation provides better performance than the Inertia Placement formulation in terms of average cost and energy usage in the controller  $u^*$ . This is expected as well because we provide more flexibility for the controller to inject/absorb energy depending on not only the node, but also on the time step. The average objective value in the Dynamic Inertia Placement formulation is 39 percent of the average optimal value of the objective function in the Inertia Placement case.

Fig. 2 and 3 show histograms of the optimal controllers  $u^*$  for the Inertia Placement formulations. Statistics in Table II show that the optimal controller for the Linear MPC formulation case uses less energy on average to maintain the frequency within the allowed bounds. Its maximum injection/absorption is between  $\pm 0.3$  p.u. (not shown in Table II). The optimal injection from the Inertia Placement formulation ranges between -2.6 and 2.8 p.u. to maintain the same safety bounds for the frequency. The control range from the Dynamic Inertia Placement is smaller (-1.2) and

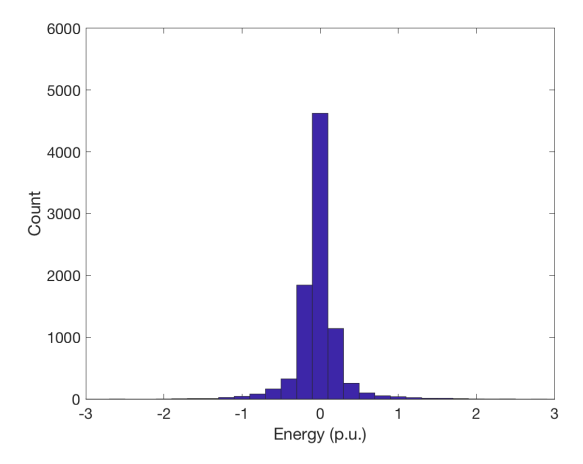


Fig. 2. Inertia Placement: Histogram of optimal controller  $u^*$  at all nodes, all time steps, and all scenarios.

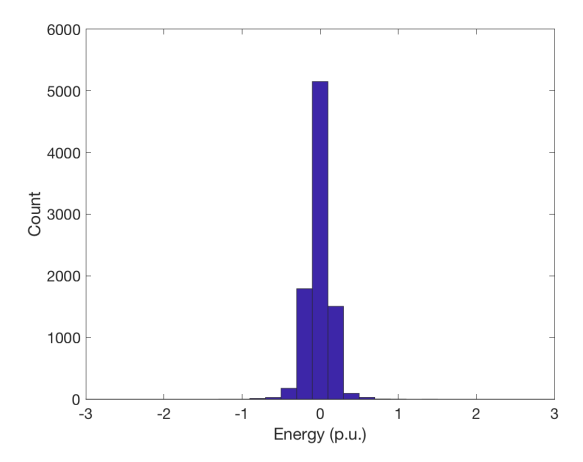


Fig. 3. Dynamic Inertia Placement: Histogram of optimal controller  $u^*$  at all nodes, all time steps, and all scenarios.

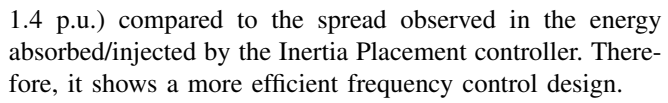


Fig. 4 and 5 show histograms of optimal costs for the Inertia Placement formulations. The moments in Table II show that the optimal values for the Linear MPC formulation are concentrated around zero. However, the Inertia Placement formulations show more spread, reaching extreme costs of 15 units (Inertia Placement) and 4.3 units (Dynamic Inertia Placement). The distribution of the costs for the Dynamic Inertia Placement controller is more skewed and its tail does not reach as high of values (Fig. 5) compared to the tale of the cost distribution in the Inertia Placement design (Fig. 4).

#### IV. CONCLUSIONS

We propose a new modeling framework for power systems dynamics that captures the variability of rotational inertia over time. Our proposed model is a Switched Affine hybrid system, whose modes change based on the change of inertia in the nodes. The transition from one mode to another is determined by a Markov Chain at each time step of the

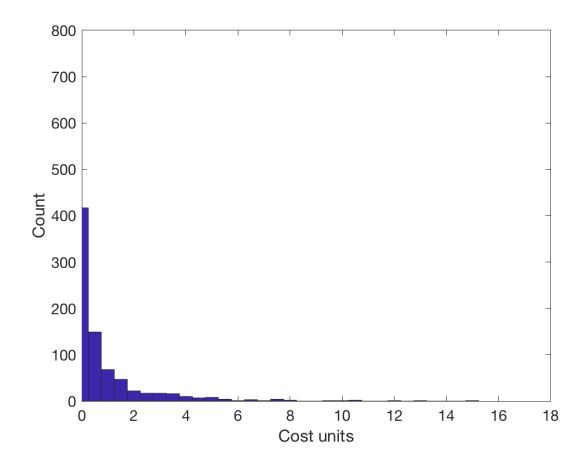


Fig. 4. Inertia Placement: Histogram of optimal cost  $J^*$  at all time steps and all scenarios.

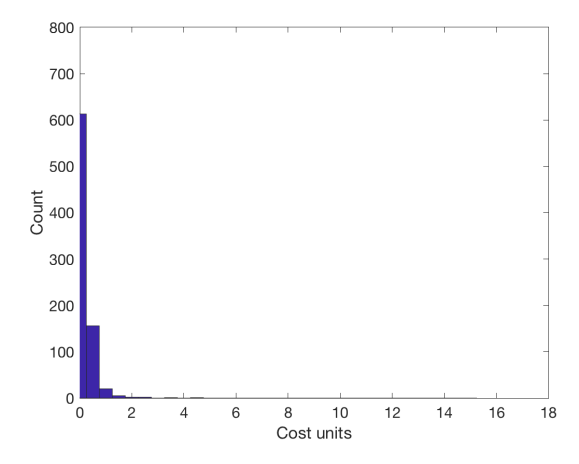


Fig. 5. Dynamic Inertia Placement: Histogram of optimal cost  $J^*$  at all time steps and all scenarios.

simulation. With this new framework, we test two standard frequency control designs and propose a third design: Linear MPC, Inertia Placement, and Dynamic Inertia Placement. As expected, the Linear MPC formulation is better in terms of cost and energy injection/absorption to control frequency. This finding encourages researchers to continue designing controllers in order to attain such optimality without having to optimize in real time (closed-loop MPC).

Another relevant finding is the fact that the Dynamic Inertia Placement proves to be more efficient in terms of cost and energy usage of the controller compared to the classical Inertia Placement case. This finding sheds light on the importance of modeling dynamics over time assuming temporal variability in the system's inertia. Additionally, it highlights the importance of designing a more flexible controller that would adapt over time. For future work we plan to study stability of the hybrid system and design a controller that is more efficient in terms of energy usage than the current virtual inertia schemes. We also plan to characterize the disturbances at each node of the network and to model the switching of modes of the hybrid system

with data-driven approaches.

#### **ACKNOWLEDGMENT**

P.H.-G. would like to thank the NSF Graduate Research Fellowships Program (GRFP). This work was also supported by NSF PIRE: Science of Design for Societal-Scale Cyber-Physical Systems (Award Number: UNIV59732), and by NSF awards 1539585 and 1646612.

#### REFERENCES

- [1] P. Kundur, "Power system stability and control," McGraw-Hill, 1994.
- [2] E. Ela, M. Milligan, and B. Kirby, "Operating reserves and variable generation," *Nat. Renew. Energy Lab., Golden, CO, USA*, Aug 2011.
- [3] J. Notenboom, P. Boot, R. Koelemeijer, and J. Ros, "Climate and Energy Roadmaps towards 2050 in north-western Europe: A concise overview of long-term climate and energy policies in Belgium, Denmark, France, Germany, the Netherlands and the United Kingdom," PBL Netherlands Environmental Assessment Agency, Netherlands, Tech. Rep., 2012.
- [4] M. Wei, J. Nelson, M. Ting, C. Yang, D. Kammen, C. Jones, A. Mileva, J. Johnston, and R. Bharvirkar, "California's carbon challenge: Scenarios for achieving 80% emissions reductions in 2050," *Lawrence Berkeley National Laboratory, UC Berkeley, UC Davis, and Itron to the California Energy Commission*, 2012.
- [5] A. Ulbig, T. S. Borsche, and G. Andersson, "Impact of low rotational inertia on power system stability and operation," *IFAC Proceedings Volumes*, vol. 47, no. 3, pp. 7290–7297, 2014.
- [6] H. Bevrani, T. Ise, and Y. Miura, "Virtual synchronous generators: A survey and new perspectives," *International Journal of Electrical Power & Energy Systems*, vol. 54, pp. 244–254, 2014.

- [7] U. Tamrakar, D. Shrestha, M. Maharjan, B. P. Bhattarai, T. M. Hansen, and R. Tonkoski, "Virtual inertia: Current trends and future directions," *Applied Sciences*, vol. 7, no. 7, p. 654, 2017.
- [8] Q.-C. Zhong and G. Weiss, "Synchronverters: Inverters that mimic synchronous generators," *IEEE Transactions on Industrial Electronics*, vol. 58, no. 4, pp. 1259–1267, 2011.
- [9] E. Mallada, "idroop: A dynamic droop controller to decouple power grid's steady-state and dynamic performance," in 2016 IEEE 55th Conference on Decision and Control (CDC), Dec 2016, pp. 4957– 4964.
- [10] A. Ulbig, T. Rinke, S. Chatzivasileiadis, and G. Andersson, "Predictive control for real-time frequency regulation and rotational inertia provision in power systems," in *Decision and Control (CDC)*, 2013 IEEE 52nd Annual Conference on. IEEE, 2013, pp. 2946–2953.
- [11] T. S. Borsche, T. Liu, and D. J. Hill, "Effects of rotational inertia on power system damping and frequency transients," in 2015 54th IEEE Conference on Decision and Control (CDC), Dec 2015, pp. 5940– 5946
- [12] B. K. Poolla, S. Bolognani, and F. Dörfler, "Optimal placement of virtual inertia in power grids," *IEEE Transactions on Automatic Control*, vol. 62, no. 12, pp. 6209–6220, 2017.
- [13] F. Borrelli, A. Bemporad, and M. Morari, "Predictive control for linear and hybrid systems," *Cambridge University Press*, 2017.
- [14] E. R. C. of Texas (ERCOT), "Future ancillary services in ERCOT," ERCOT: Taylor, TX, USA, 2013.
- [15] M. Grant and S. Boyd, "CVX: Matlab software for disciplined convex programming, version 2.1," http://cvxr.com/cvx, Mar. 2014.
- [16] —, "Graph implementations for nonsmooth convex programs," in *Recent Advances in Learning and Control*, ser. Lecture Notes in Control and Information Sciences, V. Blondel, S. Boyd, and H. Kimura, Eds. Springer-Verlag Limited, 2008, pp. 95–110.
- [17] J. Löfberg, "Yalmip: A toolbox for modeling and optimization in matlab," in *In Proceedings of the CACSD Conference*, Taipei, Taiwan, 2004